International Journal of Basic and Applied Chemical Sciences ISSN: 2277-2073 (Online)
An Open Access, Online International Journal Available at http://www.cibtech.org/jcs.htm
2018 Vol. 8(3) July-September, pp.1-21/Shukla et al.
Research Article

SYNTHESIS, CHARACTERIZATION, ANTIBACTERIAL SCREENING AND CATALYTIC ACTIVITY OF SCHIFF BASE DERIVATIVES OF TITANIUM(IV) IN THE RING-OPENING POLYMERIZATION OF Ɛ-CAPROLACTONE

***Satyendra N. Shukla, Pratiksha Gaur, Dimple Dehariya, Preeti Vaidya, Bhaskar Chaurasia, Sangeeta Jhariya**
Coordination Chemistry Research Lab, Department of Chemistry, Government Science College, Jabalpur (M.P.) 482001, India
**Author for Correspondence: ccrl_2004@rediffmail.com*

ABSTRACT
Three Schiff base ligands were synthesized by simple condensation of *o*-phenylenediamine and *o*-hydroxyacetophenone/ salicylaldehyde/ acetophenone in 1: 2 molar ratio. These ligands on reaction with $TiCl_4$ yielded three complexes of formula [Ti(*o*-HACPHEN)Cl_2], (**1);** [Ti(SALPHEN)Cl_2], (**2)** and [Ti(ACPHEN)Cl_4], (**3**). The synthesized ligands and complexes were characterized on the basis of elemental analysis, molar conductance, magnetic susceptibility, ESI-MS, electronic spectra, FT-IR,^{1}H-NMR and ^{13}C-NMR spectroscopy. Theoretical computations were carried out by Gaussian 09 software package using density functional theory (DFT) method to optimize the geometry of the investigated compounds. Additionally, bond lengths, bond angles, molecular electrostatic potential map (MEP), HOMO, LUMO, NBO charge and Mulliken charge analysis have also been performed. Complexes were scanned for catalytic activity in the synthesis of biodegradable polymer polycaprolactone from ε-caprolactone by ring-opening polymerization. Synthesized ligands and complexes were also screened for biological activity against bacteria *E. coli*.

Keywords: *Titanium complex; Schiff base ligand; Biodegradable polymer; Ring opening polymerization; Antibacterial activity; DFT study*

INTRODUCTION
Schiff base ligands are most favourite ligands used recently, due to their diverse application and simplicity of preparation. Schiff base metal-supported complexes have manifested a wide range of applications (Che and Huang, 2003; Yamada, 1999). Schiff base complexes such as Zn (Chen *et al.*, 2006), Mg (Hung and Lin, 2009), Ca (Chen *et al.*, 2007), alkali metals and transition metals (Lu *et al.*, 2012) have been used in the ring-opening polymerization (ROP) of cyclic esters, such as rac-lactide (rac-LA) and ε-caprolactone (ε-CL) and the effectiveness of Schiff base ligands in protecting the catalytic center from trans-esterification and enhancing reactivity has been widely demonstrated. Biodegradable polyesters are commonly employed in the encapsulation and delivery of proteins, the formation of hydrogels and various medicinal applications including the development of microspheres and drug delivery systems (Ha and Gardella, 2005). Metal residing within the polymer must be taken into consideration in applications involving biomaterials. As a result, non-cytotoxic metal complexes such as titanium complexes (Patel *et al.*, 2008) have been widely studied in connection with ε-CL polymerization.
In recent years metal complexes have been widely studied for their anticancer and antimicrobial (Aderoju *et al.*, 2012) properties. Furthermore, with the prevalence of drug resistance in bacterial strains metal complexes have attained great importance as antimicrobial agents (Kamalakannan and Venkappayya, 2002). However, some complexes are also reported as carbonic anhydrase inhibitor and shown strong antiglaucoma properties on the tropical application (Scozzafava *et al.*, 2011).
In view of the above facts, it will be interesting to prepare Schiff base ligands by condensation of carbonyl moiety of *o*-hydroxyacetophenone/ salicylaldehyde/ acetophenone with *o*-phenylenediamine and to synthesize its Ti(IV) complexes. The resulting ligands and complexes will be characterized by the

spectroscopic methods. In anticipation of good catalytic and biological activity, complexes will also be screened for their catalytic and antibacterial activity. However, since DFT is a simulated quantum mechanical calculation technique which provides information about compounds before its synthesis in the lab, we are also interested in optimizing the structure of the resulting ligand and complexes by DFT.

MATERIALS AND METHODS

Commercially available chemicals $TiCl_4$, *o*-phenylenediamine, *o*-hydroxyacetophenone, salicylaldehyde, acetophenone (E. Merck), ε-caprolactone (Himedia) were used as received. Tetrahydrofuran, dichloromethane, acetone, dimethyl sulfoxide (All E. Merck) and Mueller Hinton Agar media (Himedia) were used as received. Solvent ethanol and methanol were used after double distillation. Elemental analysis was estimated on Euro Vector E-3000 elemental analyzer and metal content wad analyzed gravimetrically by the literature procedure (Jeffery *et al.,* 1989). Conductivity measurements were carried out in DMSO at 25 °C on an EI-181 conductivity bridge with dipping type cell. ESI-MS spectra were recorded on Agilent - 6520(Q-TOF) mass spectrometer. FT-IR spectra were recorded in KBr pellets on Shimadzu-8400 PC spectrometer. Electronic absorption spectra were recorded in the range 800-200 nm with an EI-2371 double beam spectrophotometer equipped with a PC. ^{1}H-NMR and the ^{13}C-NMR spectrum were recorded in DMSO-d_6 on a Bruker Avance 400 (FT NMR) spectrophotometer at 400 MHz.

Synthesis of ligands and complexes

Synthesis of Schiff base ligand, (6E,7E)-N^1,N^2-bis(2-hydroxy-1-phenylethylidene)benzene-1,2-diamine;(o-HACPHEN), ***L_1***

o-Hydroxyacetophenone (2.407 mL, 0.02 mol) and *o*-phenylenediamine(1.081 g, 0.01 mol) were mixed in 30 mL ethanol and stirred for 1 h. Thereafter, reaction mixture was refluxed for 8 h. Progress of the reaction was monitored by TLC. A dark brown precipitate was obtained after cooling. It was recrystallized from hot ethanol, to obtain dark brown crystal, which was dried under vacuum. Colour = dark brown, Yield: 2.512 g (72%); m.p. = 178 °C; Anal. Calc. for $\mathbf{C_{22}H_{20}N_2O_2}$ (Mτ = 344.15): C, 76.72; H, 5.85; N, 8.13. Found: C, 76.70; H, 5.82; N, 8.08. Selected infrared absorption (KBr, cm^{-1}): ν(O-H) 3454(w); ν(C=N) 1610(s); ν(C-O) 1251(s). Electronic spectra (λ_{max} in nm) in DMSO: 380 (n→ π*), 280 (π→ π*). ^{1}H-NMR spectra (δ value in ppm): $\delta(O\text{-}H)_{phenolic}$, 14.994(s, 2H); $\delta(Ar\text{-}H)_{phenylene}$, 6.589(t, 2H); 6.627(d, 4H); $\delta(Ar\text{-}H)_{phenolic}$, 6.921(m, 2H); 7.384(t, 2H); 7.748(d, 4H); $\delta(\text{-}CH_3)$, 3.343(s, 6H). ^{13}C-NMR spectra (δ value in ppm): $\delta(>C{=}N)_{imine}$,173.27; δ(C-OH),161.67; $\delta(Ar\text{-}C)_{phenylene}$,119.81($C_1$), 115.09($C_2$), 117.91($C_3$), 116.70($C_4$), 117.46($C_5$), 116.19($C_6$); $\delta(Ar\text{-}C)_{phenolic}$,139.79($C_1$), 125.83($C_2$), 131.84($C_3$), 129.62($C_4$), 121.31($C_5$), 132.80($C_6$); $\delta(\text{-}CH_3)$,17.00. ESI-Mass spectra, m/z: $[C_{14}H_{12}NO + H^+]^+$ = 211.1123, $[C_{22}H_{20}N_2O_2 + H^+]^+$ = 345.1595, Mτ = 344.15.

Synthesis of Schiff base ligand (6E,7E)-N^1,N^2-bis(salicylidene)benzene-1,2-diamine; (SALPHEN), L_2

Salicylaldehyde (2.123 mL, 0.02 mol) and *o*-phenylenediamine (1.081 g, 0.01mol) were mixed in 30 mL ethanol and stirred for 1 h. Thereafter, the reaction mixture was refluxed for 6 h. A dark yellow precipitate was obtained after cooling, which was filtered, recrystallized from hot ethanol and dried under vacuum. Colour = dark yellow, Yield: 2.526 g (78.87%); m.p. = 150 °C; Anal. Calc. for $\mathbf{C_{20}H_{16}N_2O_2}$ (Mτ = 316.12): C, 75.93; H, 5.10; N, 8.86. Found: C, 75.89; H 5.08; N, 8.75. Selected infrared absorption (KBr, cm^{-1}): ν(O-H) 3327(w); ν(C=N) 1614(s); ν(C-O) 1276(s). Electronic spectra (λ_{max} in nm in DMSO): 360 (n→π*), 300 (π→π*). ^{1}H-NMR spectra (δ value in ppm): $\delta(O\text{-}H)_{phenolic}$, 12.937(s, 2H); $\delta(>C{=}N)_{azomethine}$, 8.931(s, 2H); $\delta(Ar\text{-}H)_{phenylene}$, 6.974(t, 2H); 6.996(d, 2H); $\delta(Ar\text{-}H)_{phenolic}$, 7.424(m, 2H); 7.679(t, 2H); 7.655(d, 4H);.^{13}C-NMR spectra (δ value in ppm): $\delta(>C{=}N)_{imine}$, 163.98; δ(C-OH),160.35; $\delta(Ar\text{-}C)_{phenylene}$, 119.70($C_1$), 119.03($C_2$), 119.45($C_3$), 119.45($C_4$), 116.63($C_5$), 119.70($C_6$); $\delta(Ar\text{-}C)_{phenolic}$,142.22($C_1$), 127.74($C_2$), 133.38($C_3$), 132.41($C_4$), 133.38($C_5$), 132.41($C_6$). ESI-Mass spectra, m/z: $[C_{13}H_{10}NO]^+$ = 196.0763, $[C_{14}H_{11}N_2O]^+$ = 223.0876, $[C_{20}H_{15}N_2O + H^+]^+$ = 300.1181, $[C_{20}H_{16}N_2O_2 + H^+]^+$ = 317.1223, Mτ = 316.12.

Research Article

Synthesis of Schiff base ligand, (6E,7E)-N^1,N^2-bis(1-phenylethylidene)benzene-1,2-diamine (ACPHEN) L_3
Acetophenone (2.333 mL, 0.02 mol) and *o*-phenylenediamine (1.081 g, 0.01mol) were mixed in 30 mL ethanol and stirred for 1 h. There after the above solution mixture was refluxed for 7 h. A dark brown precipitate was obtained after cooling, which was filtered, recrystallized from hot ethanol and dried under vacuum to yield dark brown crystal**.** Colour = dark brown, Yield: 2.55 g (74.78%); m.p. = 170 °C. Anal. Calc. for $\mathbf{C_{22}H_{20}N_2}$ (Mτ = 312.16): C, 84.58; H, 6.45; N, 8.97. Found: C, 84.51; H, 6.40; N 8.91. Selected infrared absorption (KBr, cm^{-1}): ν(C=N) 1616(s). Electronic spectra (λ_{max} in nm) in DMSO: 340 (n→ π*), 280 (π→ π*). ^{1}H-NMR spectra (δ value in ppm): δ(Ar-H)$_{phenylene}$, 6.998(t, 2H); δ(Ar-H)$_{phenolic}$, 7.466(d, 2H); 7.664(d, 4H); 7.679(t, 2H); 7.671(t, 4H); δ(-CH_3), 3.339(s, 6H). ^{13}C-NMR spectra (δ value in ppm): δ(>C=N)$_{imine}$, 164.25; δ(Ar-C)$_{phenylene}$,139.03(C_1), 129.29(C_2), 128.95(C_3), 131.11(C_4), 127.82(C_5), 128.22(C_6); δ(Ar-C)$_{phenolic}$, 144.80(C_1), 123.66(C_2), 128.69(C_3), 130.01(C_4), 124.63(C_5), 150.75(C_6); δ(-CH_3),16.09. ESI-Mass spectra, m/z: $[C_8H_8N]^+$ = 118.0660, $[C_{14}H_{12}N]^+$ = 194.0974, $[C_{16}H_{15}N_2]^+$ = 235.1245, $[C_{21}H_{18}N_2 + H^+]^+$ = 298.1538, $[C_{22}H_{20}N_2 + H^+]^+$ = 313.1641, Mτ = 312.16.

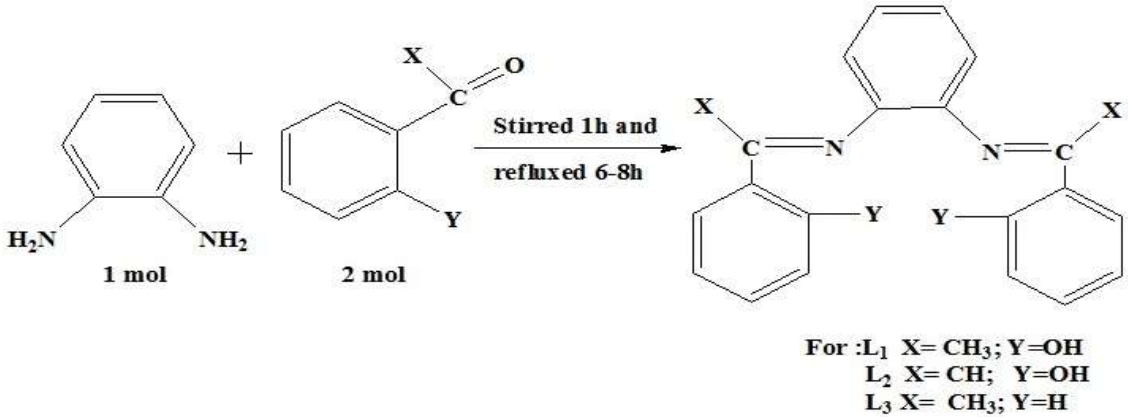

Scheme 1: Synthesis of Schiff base Ligands

Synthesis of Titanium Complexes [Ti(o-HACPHEN)Cl_2]; 1
Recrystallized Schiff base ***o*-HACPHEN** (L_1)**,** (0.344 g, 0.001mol) dissolved in 15 mL THF was mixed with solution of $TiCl_4$ (0.109 mL, 0.001 mol) in 15 mL ethanol, in a two neck flat bottom flask with continuous stirring. The resulting mixture was kept under stirring for 1 h in an inert atmosphere. A brownish black precipitate was appeared immediately in solution mixture. The mixture was refluxed till all the dark brownish black solid had been replaced by the black microcrystalline solid. After removing the solvent by filtration, the microcrystalline solid was washed several times with 1: 1, acetone: water (v/v), recrystallized from hot ethanol and dried under vacuum. Colour = Black, Yield: 0.330 g (73.0%); m.p. > 300 °C; Anal. Calc. for $\mathbf{C_{22}H_{18}Cl_2N_2O_2Ti}$ (Mτ = 461.1648): C, 57.30; H, 3.93; N, 6.07; Ti, 10.38. Found: C, 57.26; H, 3.89; N 6.01, Ti, 10.30. Molar conductance Λ_m at 25 °C (Ω^{-1} cm^2 mol^{-1}): 7 in DMSO. Selected infrared absorption (KBr, cm^{-1}): ν(C=N) 1599(s); ν(C-O) 1301(m); ν(M-O) 520(m). Electronic spectra (λ_{max} in nm) in DMSO: 450 (n→ π*), 300 (π→ π*). ^{1}H-NMR (δ value in ppm): δ(Ar-H)$_{phenylene}$, 6.939(m, 2H), 6.846(d, 2H); δ(Ar-H)$_{phenolic,}$7.914(m, 2H), 7.843(m, 2H), 7.630(d, 2H), 7.320(d, 2H); δ(-CH_3), 2.813(s,6H).^{13}C-NMR spectra (δ value in ppm): δ(>C=N)$_{imine}$, 160.76; δ(C-O),153.67; δ(Ar-C)$_{phenylene}$,113.54-127.31; δ(Ar-C)$_{phenolic}$, 128.09-153.67; δ(-CH_3),12.31.ESI-Mass spectra, m/z: $[C_{14}H_{11}Cl_2NOTi + H^+]^+$ = 327.9731, $[C_{22}H_{18}N_2O_2 + 3H^+]^+$ = 345.1465, $[C_{22}H_{18}Cl_2N_2O_2Ti + H^+]^+$ = 462.0258, Mτ = 461.02.

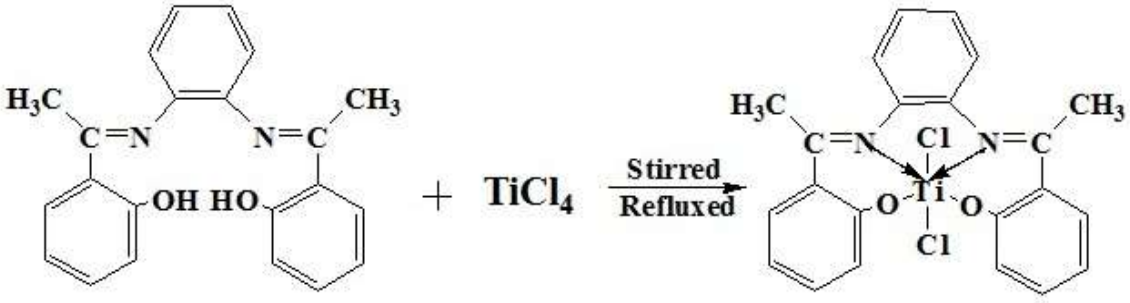

Scheme 2: Synthesis of complex 1

Synthesis of Titanium Complexes [Ti(SALPHEN)Cl_2]; 2

Recrystallized Schiff base **SALPHEN** (L_2)**,** (0.316 g, 0.001 mol) dissolved in 15 mL THF was mixed with solution of $TiCl_4$ (0.109 mL, 0.001 mol) in 15 mL ethanol in a two neck flat bottom flask with continuous stirring. The resulting mixture was stirred for 1 h in an inert atmosphere. An orange precipitate was appeared immediately in solution. The solution mixture was refluxed till all the dark orange solid had been replaced by the dark orange crystalline solid. After filtration, solid was washed several times with 1: 1, acetone: water (v/v) solution mixture, recrystallized from hot ethanol and dried under vacuum. Colour = dark orange, Yield: 0.291 g (68.5%); m.p. > 300 °C; Anal. Calc. for **$C_{20}H_{14}Cl_2N_2O_2Ti$** (Mτ = 431.9912): C, 55.46; H, 3.26; N, 6.47; Ti, 11.05. Found: C, 57.41; H, 3.20; N, 6.43; Ti, 10.95. Molar conductance $\Lambda_m$at 25 °C (Ω^{-1} cm^2 mol^{-1}): 9 in DMSO. Selected infrared absorption (KBr, cm^{-1}): ν(C=N) 1602 (m); ν(C-O) 1317(m); ν(M-O) 522(s). Electronic spectra (λ_{max} in nm) in DMSO: 330 (n→ π*), 290 (π→ π*). ^{1}H-NMR spectra (δ value in ppm): δ(>C=N)$_{imine}$, 8.645(s, 2H); δ(Ar-H)$_{phenylene}$, 6.707(m, 2H); 6.890(d, 2H); δ(Ar-H)$_{phenolic}$, 6.999(m, 2H); 7.541(m, 2H); 7.775(d, 4H);.^{13}C-NMR spectra (δ value in ppm): δ(C-O), 162.97; δ(>C=N)$_{imine}$, 159.84; δ(Ar-C)$_{phenylene}$, 113.49-121.20; δ(Ar-C)$_{phenolic}$, 125.32-154.66. ESI-Mass spectra, m/z: $[C_7H_5NO]^+$ = 119.0412, $[C_{13}H_9Cl_2NOTi + H^+]^+$ = 313.9995, $[C_{20}H_{14}N_2O_2 + 3H^+]^+$ = 317.3411, $[C_{20}H_{14}N_2O_2Ti]^+$ = 363.0520, $[C_{20}H_{14}Cl_2N_2O_2Ti + H^+]^+$ = 432.9911, Mτ = 431.99.

Syntheses of Titanium Complexes [Ti(ACPHEN)Cl_4]; 3

Recrystallized Schiff base **ACPHEN** (L_3)**,** (0.312 g, 0.001 mol) in 15 mL THF was added in to$TiCl_4$ (0.109 mL, 0.001 mol) in 15 mL ethanol in a two neck flat bottom flask with vigorous stirring. The resulting mixture was stirring for 1 h in an inert atmosphere. A dark brown precipitate was formed immediately in solution mixture. The mixture was refluxed till all the dark brown solid had been replaced by the dark brown crystalline solid. After removing the solvent by filtration, the solid was washed several times with acetone/water (1: 1), recrystallized from hot ethanol and dried under vacuum. Colour = dark brown, Yield: 0.275 g (65.3%); m.p. > 300 °C; Anal. Calc. for **$C_{22}H_{20}Cl_4N_2Ti$** (Mτ = 499.9862): C, 52.63; H, 4.02; N, 5.58; Ti, 9.53. Found: C, 52.60; H, 3.99; N, 5.53; Ti, 9.49. Molar conductance Λ_m at 25 °C (Ω^{-1} cm^2 mol^{-1}): 13 in DMSO. Selected infrared absorption (KBr, cm^{-1}): ν(C=N) 1552(s). Electronic spectra (λ_{max} in nm) in DMSO: 440 (n→ π*), 300 (π→ π*). ^{1}H-NMR (δ value in ppm): δ(Ar-H)$_{phenylene}$, 6.954(m, 2H), 6.824(d, 2H); δ(Ar-H)$_{phenolic,}$ 7.887(m, 2H), 7.829(m, 2H), 7.655(d, 2H), 7.278(d, 2H); δ(-CH_3), 2.963(s,6H). ^{13}C-NMR spectra (δ value in ppm): δ(>C=N)$_{imine}$, 159.44; δ(Ar-C)$_{phenylene}$,115.57-137.41; δ(Ar-C)$_{phenolic}$, 138.49-170.76; δ(-CH_3), 11.47. ESI-Mass spectra, m/z: $[C_8H_8ClN]^+$ = 153.0361, $[C_{14}H_{12}Cl_3NTi + 2H^+]^+$ = 348.9548, $[C_{22}H_{20}N_2Ti + H^+]^+$ = 361.1127, $[C_{22}H_{20}Cl_2N_2Ti]^+$ = 430.0518,$[C_{22}H_{20}Cl_4N_2Ti + H^+]^+$ = 500.9967, Mτ = 499.99.

Computational Study

The theoretical calculation manifested by Gaussian 09 (Frisch *et. al.*, 2010) software package was performed. Geometries of ligands and complexes were optimized by DFT, B3LYPmethod (Becke, 1993)

which is the hybrid of Becke's three-parameter exchange functional with the Lee-Yang-Parr correlation functional. The optimized structural parameters such as bond lengths, bond and dihedral angles of all the compounds were determined with the atom numbering scheme of the molecule. The HOMO, LUMO energy distributions and HOMO–LUMO energy gap of the all compounds has been calculated using the TD-SCF, DFT with 6-311++G(d, p)/ LANL2DZ basic set of the B3LYP level of theory. The energy distribution on atoms presented by Mulliken charges and natural population charges (Maurya *et al.*, 2014) as well as molecular electrostatic potential (MEP) maps were deduced using the same method.

Catalytic Activity

Complex **1-3** has been screened for the ring opening polymerization of ε-caprolactone using the complex as catalytic initiators (Scheme 3). In each set of experiment, 0.1 mmol of the complex was added to 0.97 mL (1.0 g, 8.8 mmol) of ε-caprolactone and the resulting mixture was heated at 125 ^{o}C for 6 h, 12 h and 24 h in a muffle furnace. After the completion of the reaction, the product was dissolved in 10 mL of chloroform and centrifuged for 10 min. Thereafter, the product was extracted with an excess of methanol and kept at the rest for a while. The white precipitate of polycaprolactone was obtained, which was filtered, washed with methanol, dried for 8-10 h under vacuum and weighed.

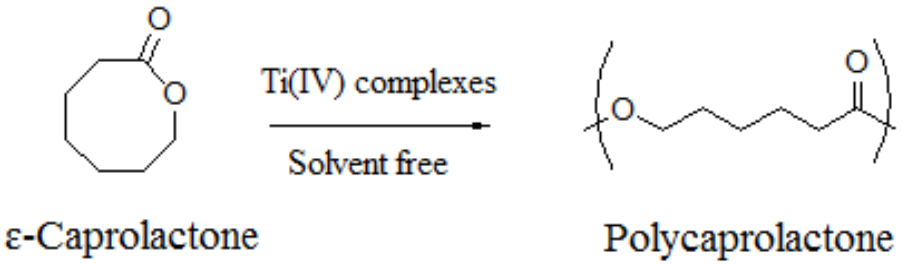

Scheme 3: Catalytic polymerization of ε-Caprolactone by Schiff base Ti complexes

Biological activity

All Schiff base ligands and complexes were screened for antibacterial activity against gram-negative bacteria *Escherichia coli* (ATCC 35218) at different concentration. Agar well diffusion method was employed for antibacterial screening (Pelczar *et al.*, 2001; Shukla *et al.*, 2008).

RESULTS AND DISCUSSION

Characterization of ligands

Empirical formulae of Schiff base ligands were in agreement with elemental analysis. The ESI-MS spectra of the ligands, $\mathbf{L_1}$, $\mathbf{L_2}$ and $\mathbf{L_3}$ exhibit several peaks depending upon the fragmentation pattern including a pseudo molecular ion peak. The ESI-MS spectra of the ligand, $\mathbf{L_1}$ (Figure 1) shows peaks at m/z: 211.1123 and 345.1595 attributed for $[C_{14}H_{12}NO + H^+]^+$and $[C_{22}H_{20}N_2O_2 + H^+]^+$respectively. The peak observed at m/z 345.1595 was due to pseudo molecular ion. ESI-MS of $\mathbf{L_2}$ exhibit peak at 196.0763, 223.0876, 300.1181 and 317.1223 attributed for $[C_{13}H_{10}NO]^+$, $[C_{14}H_{11}N_2O]^+$, $[C_{20}H_{15}N_2O + H^+]^+$ and $[C_{20}H_{16}N_2O_2 + H^+]^+$. The peak at 317.1223 was due to $[M + H^+]^+$, a pseudo molecular ion. ESI-MS of $\mathbf{L_3}$ exhibit peak at 118.0660, 194.0974, 235.1245, 298.1538 and 313.1641 assigned for $[C_8H_8N]^+$, $[C_{14}H_{12}N]^+$, $[C_{16}H_{15}N_2]^+$, $[C_{21}H_{18}N_2 + H^+]^+$and $[C_{22}H_{20}N_2 + H^+]^+$. A peak at 313.1641 was due to $[M + H^+]^+$ pseudo molecular ion.

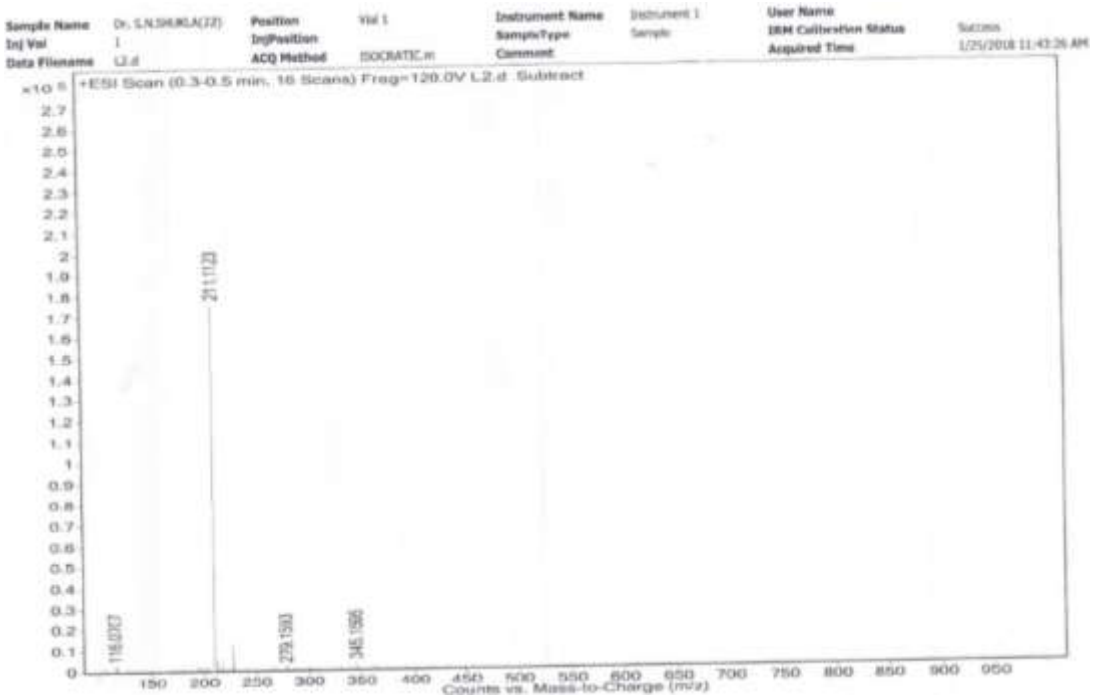

Figure 1: ESI-Mass spectra of ligand L_1

FT-IR spectra of ligands $\mathbf{L_1}$ and $\mathbf{L_2}$ exhibits a peak at 3454 and 3327 cm^{-1}respectively, due to ν(O-H) stretching vibration. This peak in $\mathbf{L_2}$ was slightly shifted to lower wave number probably due to H-bonding in hydroxyl. All ligands exhibit a peak of sharp intensity in between 1610-1614 cm^{-1}, attributed to the ν(C=N) azomethine/imine group. $\mathbf{L_1}$ and $\mathbf{L_2}$ show a peak between 1251-1276 cm^{-1} assigned for ν(C-O) bond (Silverstein *et. al*., 1991). FT-IR of $\mathbf{L_1}$ is given in Figure 2.

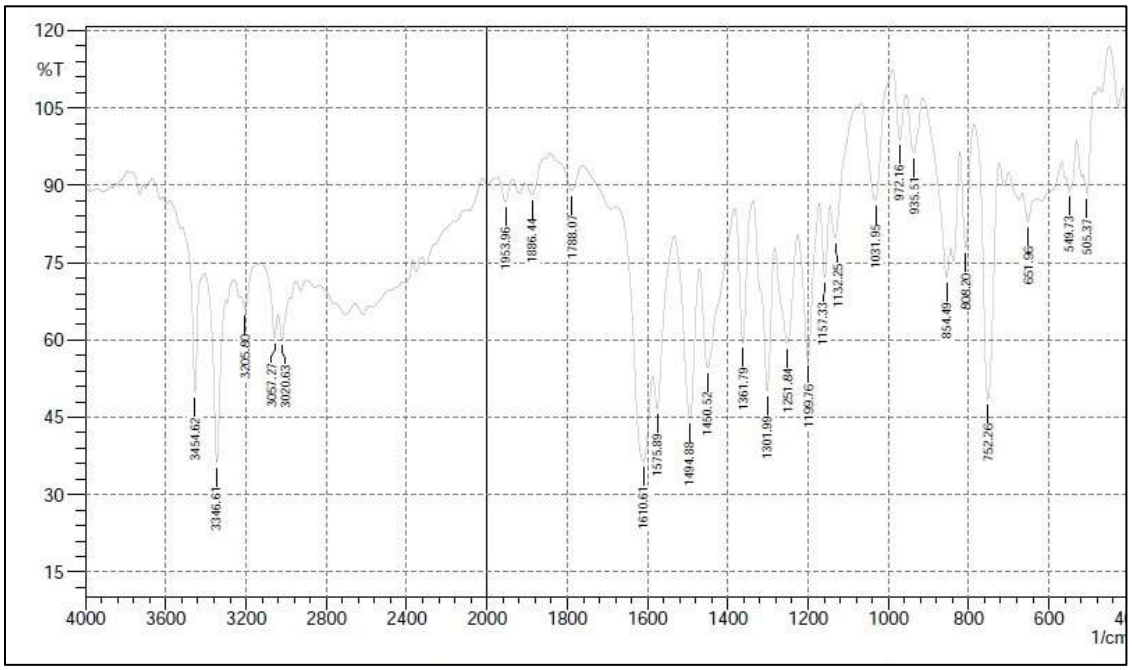

Figure 2: FT-IR Spectra of ligand L_1.

UV–Vis spectra of ligands exhibit two absorption bands at ~ 300 nm and ~ 360 nm. The first band of high extinction was assigned to π→ π* transition associated with the aromatic ring. Another band of medium intensity at ~ 360 nm, was attributed to n→ π*transition for (C=N) imine nitrogen. Electronic spectra of ligand $\mathbf{L_1}$ is given in Figure 3.

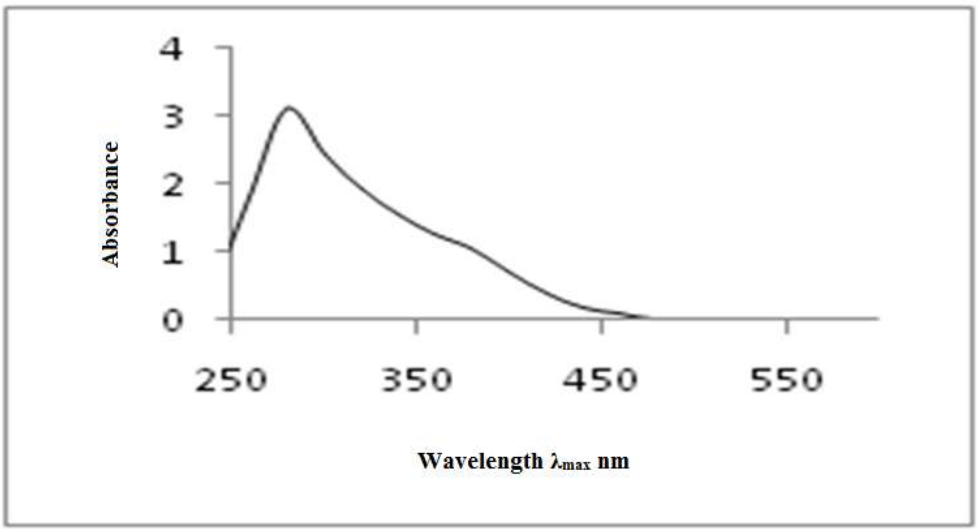

Figure 3: UV-Vis spectra of L_1

In ^{1}H-NMR spectra of $\mathbf{L_1}$, a triplet centred at ~ δ 6.607 ppm and a doublet centred at ~ δ 6.683 ppm for two protons each were assigned for four protons of phenylene moiety. A doublet centred at ~ δ 6.799 ppm, multiplet centred at ~ δ 6.930 ppm, a triplet centred at ~ δ 7.384 ppm and a doublet centred at ~ δ 7.748 ppm for two protons each, were attributed for all the eight aromatic protons of the phenolic moiety. In $\mathbf{L_2}$ a triplet centred at ~ δ 6.974 ppm was attributed for four phenylene proton. A multiplet centred at ~ δ 7.424 ppm for six protons and a double doublet centred at ~ δ 7.679 ppm for two protons were assigned to the phenolic moiety. In $\mathbf{L_3}$ a triplet centred at ~ δ 6.998 ppm and a doublet centred at ~ δ 7.466 ppm for two protons each, were attributed for four phenylene proton. A doublet centred at ~ δ 7.664 ppm for four protons, a triplet centred at ~ δ 7.679 ppm for two protons and a triplet centred at ~ δ 7.671 ppm for four protons were attributed for all the ten aromatic protons of the two phenyl moiety. In $\mathbf{L_1}$ and $\mathbf{L_2}$ singlet observed at δ 14.994 ppm and δ 12.937 ppm respectively, for two protons each, was assigned for phenolic (-OH) group. In $\mathbf{L_2}$ singlet observed at δ 8.931 ppm attributed to two protons of azomethine moiety. In $\mathbf{L_1}$ and $\mathbf{L_3}$ singlet observed at δ 3.343 ppm and δ 3.339 ppm respectively, for six protons was attributed for methyl group attached to azomethine nitogen.^{1}H-NMR Spectrum of the $\mathbf{L_1}$ is shown in Figure 4.

The number of signals of sharp peaks represented the number of carbons of the compound which are chemically non-equivalent. The ^{13}C-NMR spectrum of ligands exhibits a signal in the range δ 163-173 ppm assigned for imine(>C=N–) carbon. In ligands signal for aromatic carbon ranges in between δ 115.00 - δ 154.00 ppm. In $\mathbf{L_1}$ and $\mathbf{L_2}$ a signal observed at ~ δ 154 ppm was attributed to phenolic carbon linked with the hydroxyl group. Phenylene carbon linked with azomethine–N exhibit signal between δ 131.00 - δ 143.00 ppm. Other aromatic carbon of phenolic moiety displayed signal between δ 115.00 - δ 129.00 ppm. In ligand $\mathbf{L_1}$ and $\mathbf{L_3}$, the signal observed at δ 17.00 ppm and δ 16.09 ppm were assigned for methyl carbons respectively. ^{13}C-NMR spectra of $\mathbf{L_1}$ is shown in Figure 5.

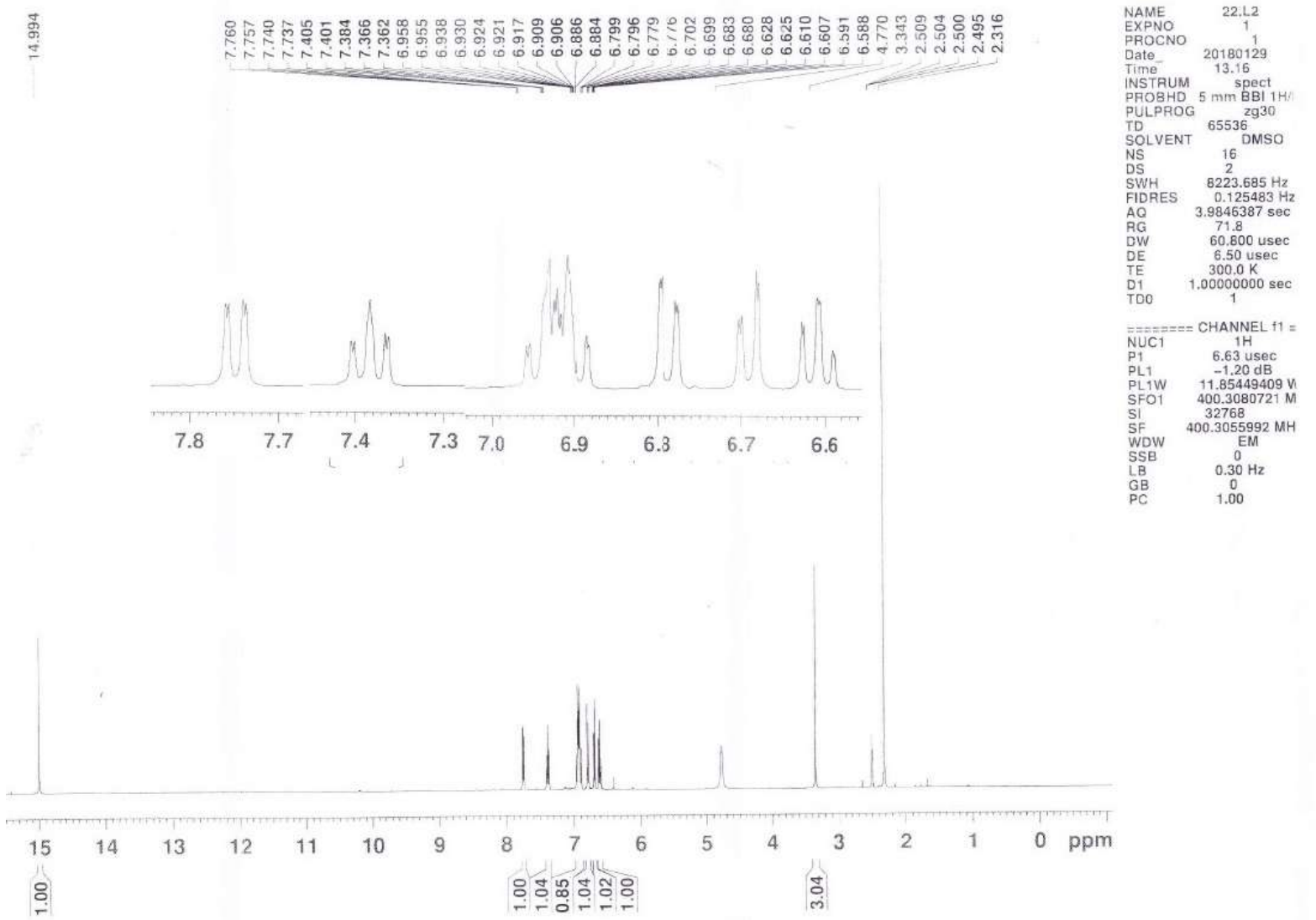

Figure 4: ^{1}H-NMR Spectra of L_1.

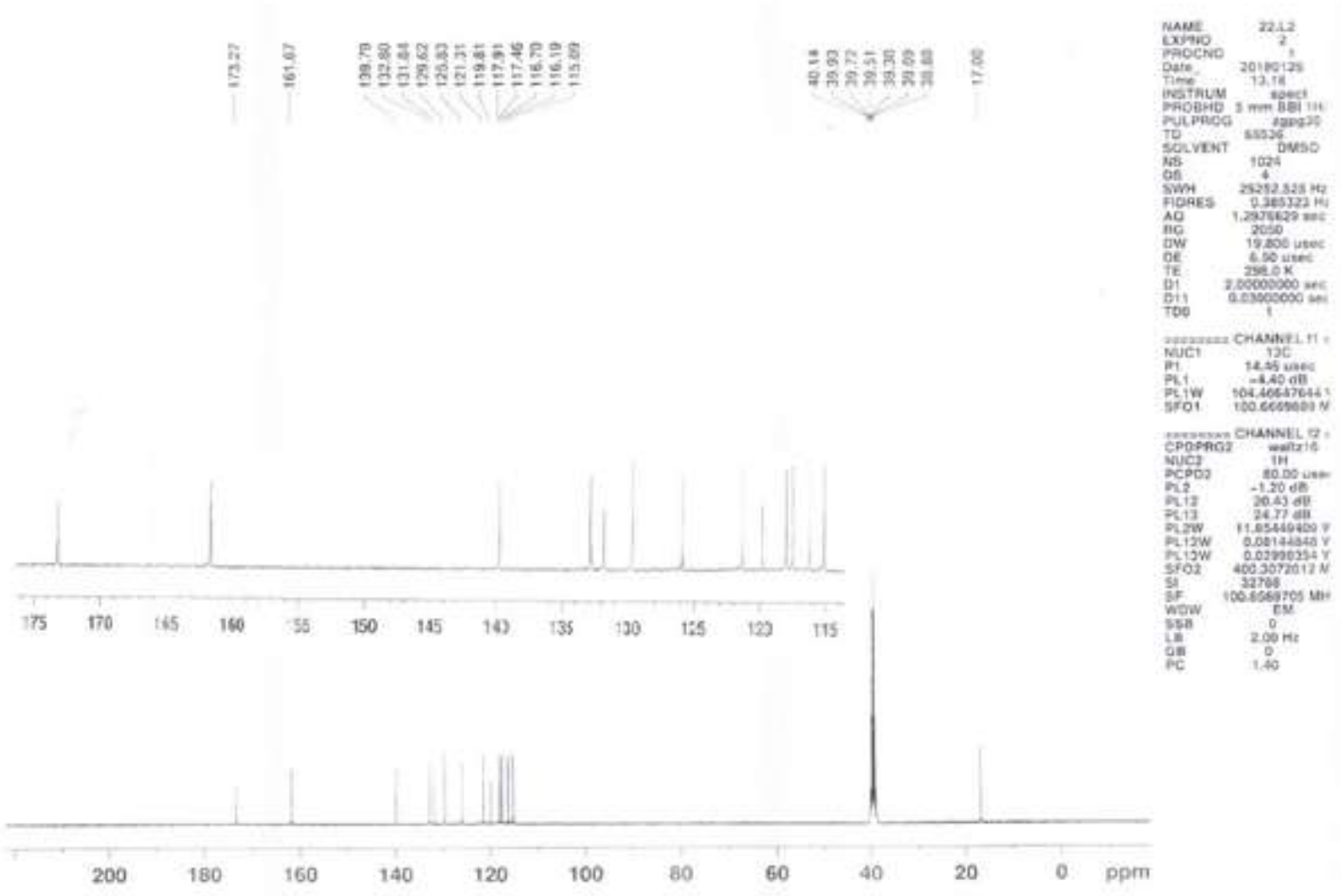

Figure 5: ^{13}C-NMR spectra of L_1

Thus on the basis of ESI-MS, FT-IR, UV-Vis, ^{1}H-NMR and ^{13}C-NMR spectroscopy following structures (Figure 6 (a), (b) and (c)) of ligands were suggested.

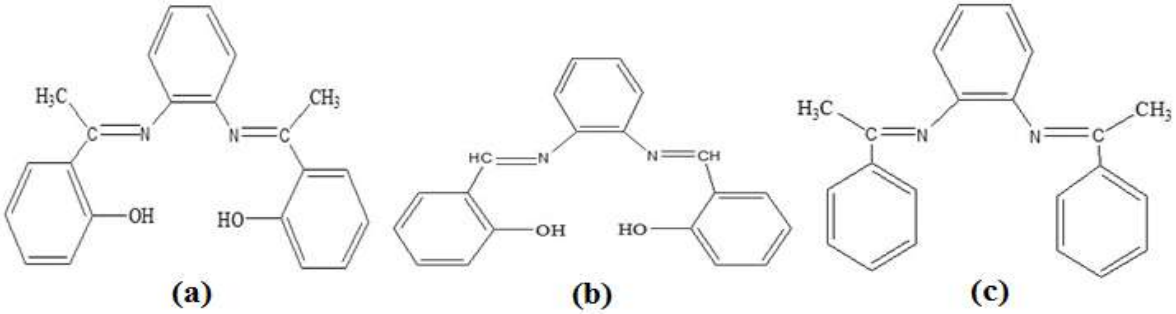

Figure 6: Structure of ligands (a) L_1, (b) L_2 and (c) L_3

Characterization of complexes

Stoichiometries of the complexes were in agreement with elemental analysis data. Molar conductance of complexes (10^{-3} M in DMSO) was in between7-13 Ω^{-1} cm^2 mol^{-1}, indicating the non-electrolytic nature of complexes (Geary, 1971). ESI-Mass spectra of all the three complexes exhibit several peaks depending upon the fragmentation pattern. Complex 1 (Figure 7) exhibit several peaks such as at m/z = 327.9731, 345.1465, and 462.0258 attributed for $[C_{14}H_{11}Cl_2NOTi + H^+]^+$, $[C_{22}H_{18}N_2O_2 + 3H^+]^+$and $[C_{22}H_{18}Cl_2N_2O_2Ti + H^+]^+$ respectively including $[M + H^+]^+$, a pseudo molecular ion peak. Complex 2 exhibits peaks at m/z = 119.0412, 313.9995, 317.3411, 363.0520 and 432.9911 attributed for $[C_7H_5NO]^+$ $[C_{13}H_9Cl_2NOTi + H^+]^+$, $[C_{20}H_{14}N_2O_2 + 3H^+]^+$, $[C_{20}H_{14}N_2O_2Ti]^+$ and $[C_{20}H_{14}Cl_2N_2O_2Ti + H]^+$respectively. A peak at m/z = 432.9911 is a pseudo molecular ion peak. However, complex 3 exhibits several peaks at m/z = 153.0361, 348.9548, 361.1127, 430.0518, and 500.9967 assigned for $[C_8H_8ClN]^+$, $[C_{14}H_{12}Cl_3NTi + 2H^+]^+$, $[C_{22}H_{20}N_2Ti + H^+]^+$, $[C_{22}H_{20}Cl_2N_2Ti]^+$ and $[C_{22}H_{20}Cl_4N_2Ti + H^+]^+$ respectively. A peak at m/z = 500.9967 is a pseudo molecular ion peak.

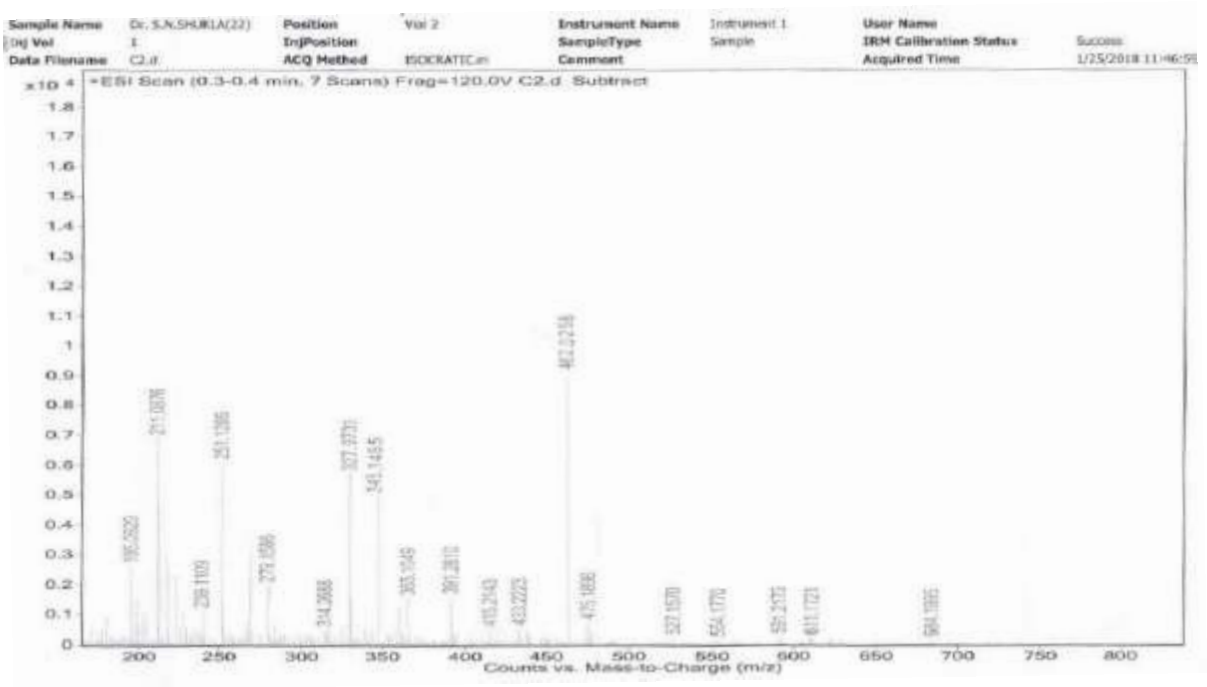

Figure 7: ESI-MS spectra of complex 1

In FT-IR spectra of complexes, a strong peak appeared in between 1610-1616 cm^{-1} in the ligands for imine ν(>C=N–) groups was shifted downwards in the complexes and observed in between 1599 - 1602 cm^{-1} indicating the coordination of imine nitrogen to the metal. In the ligands $\mathbf{L_1}$and $\mathbf{L_2}$, a band of medium to low intensity appeared at 3454 cm^{-1} and 3327 cm^{-1} respectively assigned to ν(O–H) vibrations, was vanished completely in the complexes and at the same time a new peak of medium intensity was appeared in complex **1** and **2,** at ~ 520 $cm^{-1}$was assigned for M–O bond stretching, indicative of the bonding of metal to the oxygen by removal of phenolic –H (Sujamol *et. al.*, 2010). Ligand $\mathbf{L_1}$ and $\mathbf{L_2}$ also show a sharp peak in between 1251 - 1276 cm^{-1}, which was shifted upward on complexation indicative of strengthening of (C-O) bond on complexation and appeared at 1301 cm^{-1} and 1317 cm^{-1} respectively, in complex **1** and **2**. FT-IR spectra of complex **1**, is given in Figure 8.

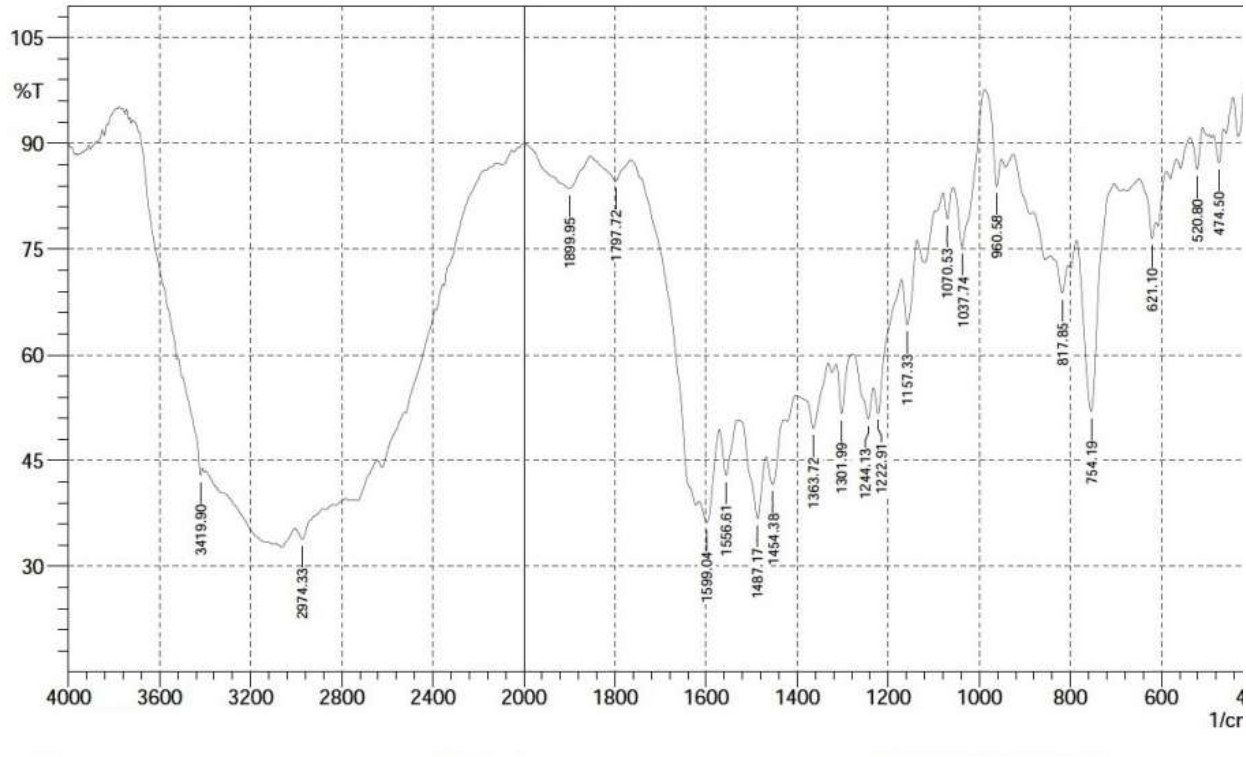

Figure 8: FT-IR spectra of complex 1

Complexes are diamagnetic as expected in Ti(IV) complexes. The electronic spectra of complexes exhibit only two bands in UV-Visible range. The band of higher extinction coefficient observed at ~ 300 nm was assigned to π→ π* transitions of ligand. Another band of medium intensity at ~ 450 nm was assigned to n→ π* transition. Shifting of this band to higher wavelength clearly indicates the transfer of electron pair from azomethine-N to metal ion (A. B. P. Lever, 1984, V. B. Badwaik and A. S. Aswar, 2007). The electronic spectrum of complex **1** is given in Figure 9.

^{1}H-NMR spectra of complex **1** and **2** exhibit nine to twelve signals in the aromatic region. This is probably because of lost of planarity in ligand on coordination, due to which almost all hydrogen has its own resonance in proton NMR. These complexes displayed two singlets centred at ~ δ 6.590 ppm and δ ~ 6.760 ppm and two multiplets at δ ~ 6.850 ppm and ~ δ 6.950 ppm for one proton each attributed to phenylene proton. Complex **1** and **2** exhibit two doublets centred at ~ 7.000 ppm and ~ 7.860 ppm and six multiplets centred at ~ δ 7.140 ppm, ~ δ 7.329 ppm, ~ δ 7.370 ppm, ~ δ 7.610 ppm, ~ δ 7.730 ppm and δ 7.920 ppm for one proton each were attributed to phenolic proton. In complex **3** a signal for azomethine

nitrogen was shifted to higher delta value indicating the transfer of an electron pair from azomethine nitrogen to the metal. In this particular complex, there are five signals in the aromatic region. In proton NMR a triplet centred at δ 6.814 ppm and a doublet centred at ~ δ 7.810 ppm for two protons each were assigned to phenylene ring linked directly to azomethine-N. Similarly, a doublet centred at ~ δ 6.610 ppm for four protons, a triplet centred at ~ δ 6.910 ppm for four protons and a multiplet centred at ~ δ 7.950 ppm for two protons were assigned for phenyl ring proton linked to azomethine carbon. In complex **1** and **3** proton NMR display two singlets at ~ δ 2.810 ppm and δ 2.790 ppm for three protons each, attributed for the two methyl groups present in the different environment. A signal observed in between δ 14.997 ppm and δ 12.937 ppm in $\mathbf{L_1}$ and $\mathbf{L_2}$ vanished in complex **1** and **2** indicating the formation of the metal-oxygen bond by replacement of hydroxyl proton.

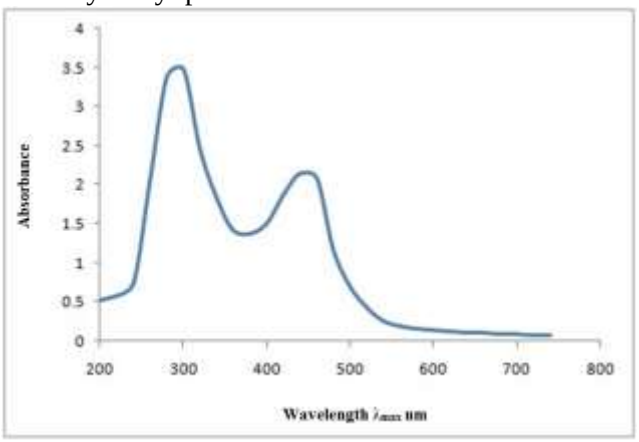

Figure 9: UV-Vis spectra of complex 1

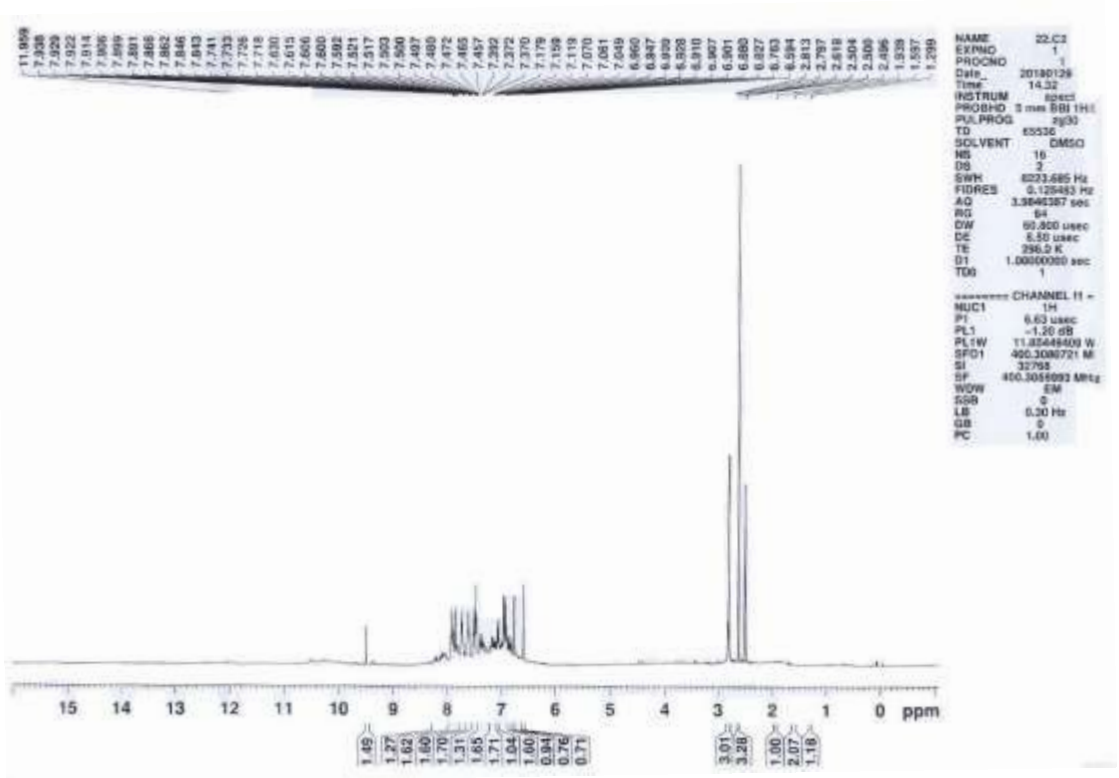

Figure 10: ^{1}H-NMR Spectra of complex 1.

Research Article

The ^{13}C-NMR spectrum of the ligands exhibit a signal between δ 163.00 - 173.00 ppm assigned for imine/ azomethine (>C=N–) carbon. This signal was shifted to lower delta value in complexes at appeared at ~ δ 160.00 ppm. Aromatic carbon display signal in the range δ 113.00- δ 153.00 ppm. In the **1** and **2,** a signal appearing at ~ δ 153.00 ppm was attributed to the carbon linked with the hydroxyl group. The signal between δ 130.00 ppm - δ 150.00 ppm were attributed to phenylene carbon. The signal between δ 113.00 - δ 129.00 ppm was attributed for the other phenolic proton. In complex **1** and **3,** the signal observed at δ 12.31 ppm and δ 11.47 ppm were assigned methyl carbons respectively. The ^{13}C-NMR spectrum of complex **1** is shown in Figure 11.

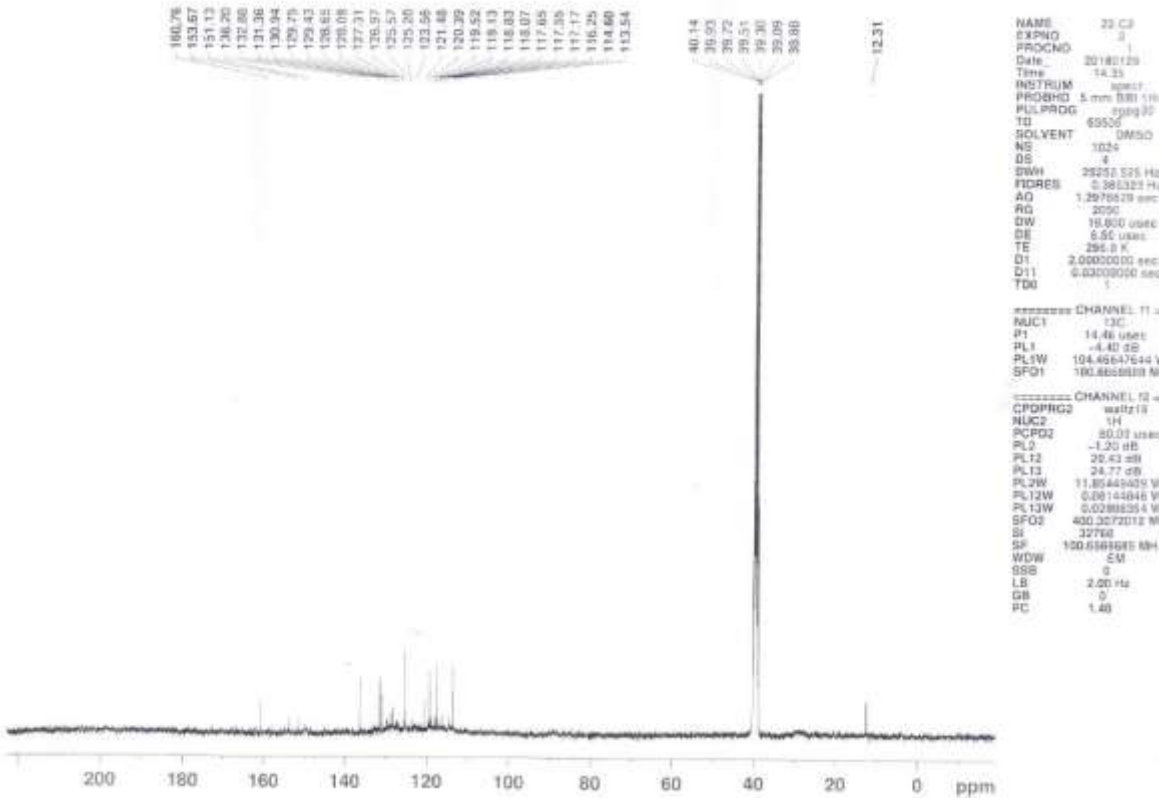

Figure 11: ^{13}C-NMR Spectra of complex 1

Thus on the basis of elemental analysis, molar conductance, ESI-MS, FT-IR, ^{1}H-NMR and ^{13}C-NMR following structure (Figure 12 (a), (b) and (c)) of complexes **1-3** were suggested.

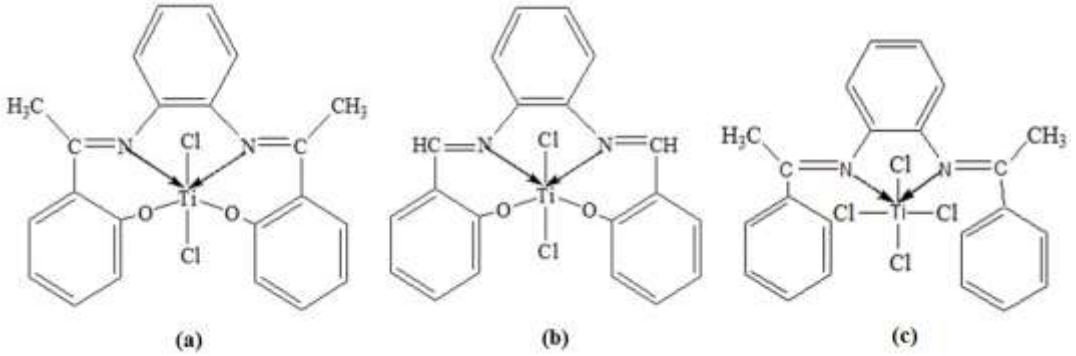

Figure 12: Structure of (a) complex 1, (b) complex 2, (c) complex 3

Quantum chemical parameters

All calculated values of the following quantum chemical parameters: the highest occupied molecular orbital energy (E_{HOMO}), the lowest unoccupied molecular orbital energy (E_{LUMO}), the difference between HOMO and LUMO energy levels, (ΔE), Mulliken electronegativity (χ), absolute hardness (η), absolute softness (σ), chemical potential (Pi), global softness (S), global electrophilicity(ω), additional electronic charge (ΔN_{max}), dipole moment (μ) and total energy (E-TD-HF/ETD-KS) after geometrical optimization of the structures of compounds were listed in Table 1. The negative values of both E_{HOMO} and E_{LUMO} were indicative of the stability of synthesized ligands and complexes. The energy gap between E_{HOMO} and E_{LUMO} of ligands **L_1 - L_3**, complex **1** and **2** were shown in Figure 13 (a), (b), (c), (d), and (e). In the compounds under investigation, some important molecular orbitals for the ligands **L_1 - L_3** and the complex **1** and **2** were selected to explain the difference that occurred to the various energy characters of ligands when bonded with metal. All ligands coordinate to metal ions through the nitrogen of azomethine/imine. However, **L_1**and **L_2** coordinate also through the deprotonated oxygen of the hydroxyl group in addition to azomethine-N. These atoms carry more charge confirming active sites for coordination. The energy difference between values of absolute softness (σ) in the Ligands and complex **1** and **2** indicates that ligands have a good tendency to chelate with a metal ion. The negative values of chemical potential (Pi) in complex **1** and **2** indicate that energy must decrease on accepting electronic charge form ligands. The value of Pi depends upon the Mulliken electronegativity (χ). The increases in the global electrophilicity(ω) value of complex **1** and **2** attributed to higher electron accepting capability (Parr *et al.*, 1999).

Table 1: Quantum chemical parameters

Parameters	*o*-HACPHEN	SALPHEN	ACPHEN	Complex 1	Complex 2
HOMO	-5.033	-5.876	-5.315	-6.393	-6.645
LUMO	-1.250	-1.913	-1.401	-4.694	-2.812
ΔE	3.783	3.962	3.914	1.699	3.832
Mulliken electronegativity χ	3.141	3.895	3.358	5.543	4.729
Global Hardness η	1.891	1.981	1.957	0.849	1.916
Absolute softness σ	0.528	0.504	0.510	1.176	0.521
Chemical Potential *Pi*	-3.141	-3.895	-3.358	-5.543	-4.729
Global Softness S	0.264	0.252	0.255	0.588	0.260
Global Electrophilicity ω	2.608	3.829	2.881	18.087	5.835
Electronic Charge ΔN	1.660	1.966	1.715	6.525	2.468
Dipole Moment μ	3.953	4.403	0.913	9.763	7.737
Total energy (a. u.)	-1109.188	-1031.213	-958.849	-1196.478	-1118.479

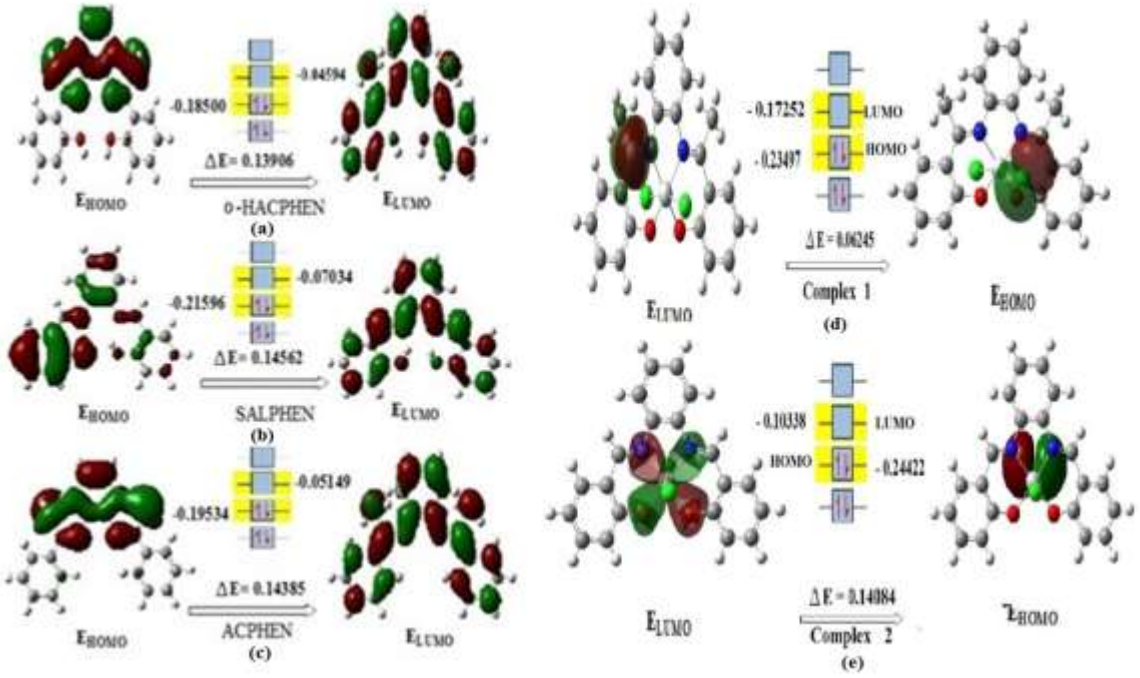

Figure 13: HOMO LUMO energy difference of (a) L_1, (b) L_2, (c) L_3, (d) Complex 1 and (e) Complex 2.

Mulliken charge analysis

The net atomic charges of ligands and complexes were obtained by means of Mulliken population analysis and natural charge population analyses of natural bond orbital (NBO). Charge distribution on a molecule has a significant influence on the vibration spectra. This calculation depicts the charges of every atom in the molecule. Distribution of positive and negative charges are the major cause to increase or decrease bond length. In the fact that, Mulliken scale is not so much reliable in such analysis, the results give a surprising difference between the Mulliken's and the NBO charge analysis. The graphical representation (Figure 14) of Mulliken charge analysis and natural charge populations of ligand $\mathbf{L_1}$shows that, the atoms C3, C4, C13, C14, C26 and C35, and all hydrogen atoms are positively charged both in NBO and Mulliken analyses. The remaining carbon atoms and some electronegative atoms such as N11, N12, O43 and O44 bear negatively charge. However, the graphical representation (Figure 14) of Mulliken charge analysis and natural charge populations of complex **1** shows that the atoms C1, C2, C13, C14, C18, C19, C27, all hydrogen atoms and Ti39 are positively charged both in NBO and Mulliken analyses. In the ligand $\mathbf{L_1}$, N11, N12, O43, O44 atoms and in complex **1** atoms such as N11, N12, O37 and O38 bears negative charges.

Bond parameters

Determination of the molecular structure of complexes in the absence of single crystal is done by DFT optimizations in the gas phase of ligands and complexes were performed. The optimized bond lengths, bond angle and dihedral angles of investigated compound calculated by B3LYP methods with 6-31++G (d,p)/LANL2DZ basis set were listed in Table 2 and 3 in accordance with atom numbering scheme as shown in Figure 15(a), (b), (c), (d), and (e). The optimized geometrical parameters of ligands are compared with complexes. The calculated C-O bond distances in ligand $\mathbf{L_1}$ and $\mathbf{L_2}$ found 1.430 Å and 1.429 Å respectively, but in complex **1** and **2**, the distance between C-O bond was observed slightly shorter than free ligands after complexation and found 1.433 Å and 1.445 Å respectively. Bond length of azomethine C=N in ligands was found at ~1.293 Å, which increases in the case of complexes and observed at ~1.281Å. This increase in bond distance was because of transfer of electron density of double

bond towards metal and decrease in the double bond character of C=N and hence increase in bond length, which in turn confirms the coordination of metal with azomethine-N. The optimized structure for the ligands and complexes were proposed in Figure 15(a), (b), (c), (d), and (e).

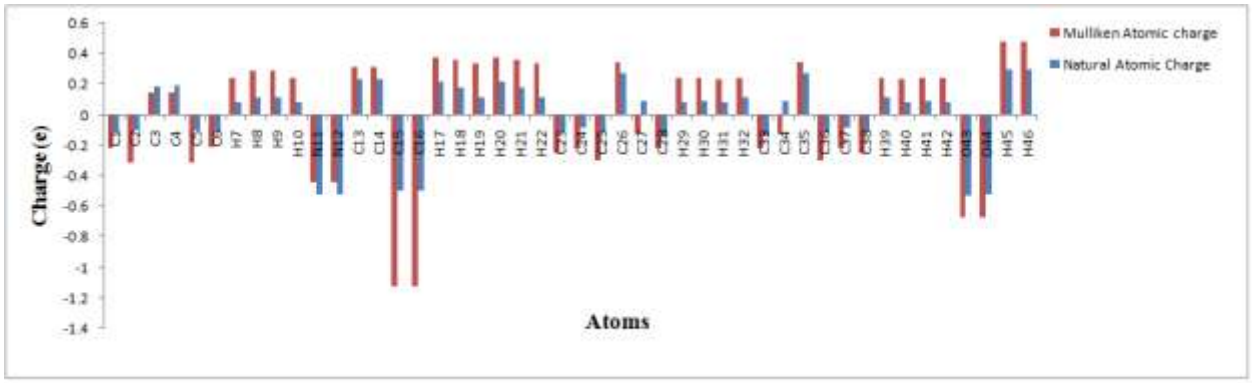

(a)

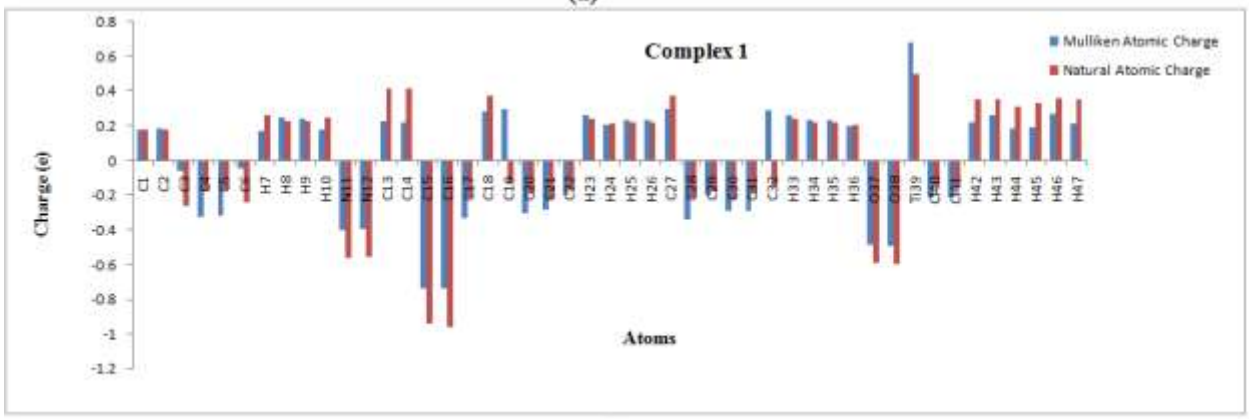

(b)

Figure 14: Mulliken charge distribution of ligand (a) L_1 and (b) complex 1

Table 2: Selected geometrical bond length of ligands and complexes

Bond Length (in Angstrom Å)				
L_1	**L_2**	**L_3**	**Complex 1**	**Complex 2**
(C35-O44) 1.430	(C17-O38) 1.429	(C14-C15) 1.540	(C18-O37) 1.433	(C12-O38) 1.445
(H46-O44) 0.960	(H39-O38) 0.962	(H34-C28) 1.070	-	-
AZOMETHINE	AZOMETHINE	AZOMETHINE	AZOMETHINE	AZOMETHINE
(C14=N12) 1.293	(C14=N12) 1.293	(C14=N12) 1.293	(C13=N12) 1.291	(C33=N31) 1.281
(C14-C15) 1.540	(H16-C14) 1.068	-	(C13-C15) 1.540	(H33-C35) 1.070
-	-	-	(O37-Ti39) 1.975	(O38-Ti37) 1.979
-	-	-	(N12-Ti39) 2.032	(N31-Ti37) 1.994
-	-	-	(Ti39-Cl40) 2.310	(Ti37-Cl40) 2.309

Table 3: Selected geometrical bond angles and dihedral angles of ligands and complexes.

Bond Angle (in Degree)				
L_1	**L_2**	**L_3**	**Complex 1**	**Complex 2**
(∠C4-N12-C14)	(∠C2- N12-C14)	(∠C15-C14-N12)	(∠C15-C13-N11)	(∠H35-C33-N31)
120.001	119.899	120.000	118.270	117.699
(∠C15-C14-N12)	(∠N12-C14-H14)	(∠C33-C28-H34)	(∠C1-N11-C13)	(∠C33-N31-Ti37)
120.000	120.039	120.000	120.280	124.640
(∠N12-C14-C34)	(∠C17-O38-H39)	(∠C2-N12-C14)	(∠C18-O37-Ti39)	(∠C12-O38-Ti37)
119.998	119.265	120.000	116.290	117.616
(∠C35-O44-H1246)	(∠C22-C14-N12)	(∠N12-C2-N1)	(∠N11-Ti39-N12)	(∠N31-Ti37-N32)
109.471	120.091	119.999	78.649	83.027
-	-	-	(∠N11-Ti39-O37)	(∠N31-Ti37-O38)
			93.639	98.819
-	-	-	(∠O37-Ti39-O38)	(∠O38-Ti37-O39)
			100.113	81.194
-	-	-	(∠Cl41-Ti39-N11)	(∠N31-Ti37-Cl40)
			81.079	82.876
Dihedral Angle (in Degree)				
(C34-C14-N12-C4)	(C2-N12-N14-C22)	(C2-N12-C14-C33)	(C1-N11-C13-C19)	(C1-N31-C33-C13)
-179.997	-178.519	-180.000	-178.440	-178.841
(H46-O44-C35-C34)	(C18-C17-O38-H39	(C1-N11-C13-C19)	(C15-C13-N11-Ti39)	(H35-C33-N31-Ti37)
149.999	-177.031	-179.998	-175.542	-176.874
-	-		(C14-N12-Ti39-O37)	(Ti37-O38-C12-C11)
			110.248	160.594
-	-		(N11-Ti39-O38-C27)	(C33-N31-Ti37-O39)
			105.784	-111.120

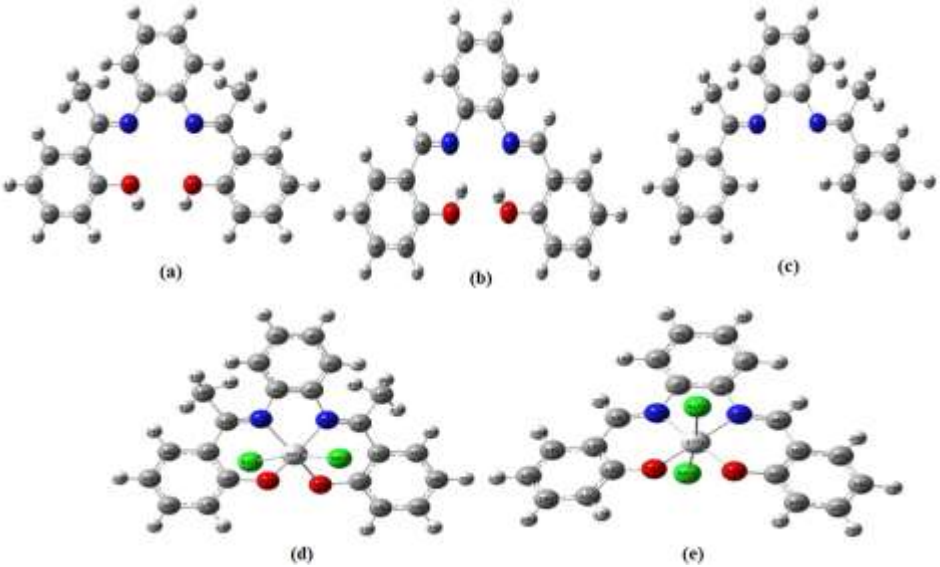

Figure 15: DFT optimized structure of (a) L_1, (b) L_2, (c) L_3, (d) complex 1, and (e) complex 2.

Molecular electrostatic potential analysis (MEP) and contour maps

The molecular electrostatic potential (MEP) is related to the electronic density and a very useful descriptor in understanding sites for electrophilic attack and nucleophilic reactions as well as hydrogen bonding interactions. The MEP mapped surface of the molecule was calculated by the B3LYP method with the 6-31++G(d,p) basis set. The MEP maps of ligand $\mathbf{L_1}$ and complex **1** were shown in Figure 16. As it can be easily observed from the MEP map of the $\mathbf{L_1}$, the negative regions in MEP are related to the electronegative site, while the positive regions are related to the electropositive site. This molecule has several possible sites for coordination. As it can be easily observed from the MEP map of the ligand, greatest negative area favoured for the electronegative reaction is shown by the red colour, while the extreme positive district favoured for the electropositive reaction is illustrated by the blue colour. The increase in the potential can be ordered as follow: blue > green > red, where blue demonstrates the powerful attraction while the red illustrates the powerful repulsion. Areas with negative values are distributed on nitrogen, oxygen and chlorine atoms while the regions having the positive values are distributed on the hydrogen atoms and the metal atom (Scrocco *et al.,* 1978). The "MEP" maps of $\mathbf{L_1}$ and its complex **1** are shown in Figure 16 (a) and (b).

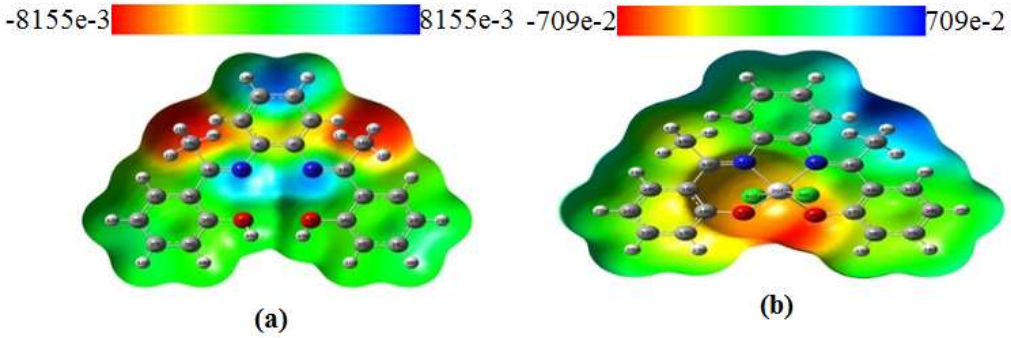

Figure 16: Molecular electrostatic potential (MEP) of (a) L_1, and (b) complex 1.

Catalytic activity

To optimize the reaction polymerization reaction was carried out with 0.1 mmol of the catalyst at 125º C for 6 h,12 h and 24 h. Results obtained were (Table 4) illustrates the degree of catalytic activity in the polymerization of ε-CL associated with complex **1-3**. It was clearly observed from the table that in all cases yields of polymerization reaction increases with time. At particular temperature of 125°C it was observed that in all complexes the highest yield was obtained after 24 h. From Table 4 it is clear that the order of catalytic efficiency of complexes is **3 > 2 > 1**. The highest yield was obtained in the case of complex **3** after 24 h.

Table 4: Polymerization of ε-Caprolactone by Ti Schiff base complex 1-3 as an initiator at 125 °C

Complexes	ε-caprolactone		Complexes		Temperature	Time	Yield		M_n- Value
	mL	mmol	gram	mmol	ºC	hour	mg	%	
	0.97	8.8	0.04	0.1	125ºC	6	0.332	33%	226986
Complex 1	0.97	8.8	0.04	0.1	125ºC	12	0.403	40%	242325
	0.97	8.8	0.04	0.1	125ºC	24	0.530	53%	287276
	0.97	8.8	0.04	0.1	125ºC	6	0.489	48%	273652
Complex 2	0.97	8.8	0.04	0.1	125ºC	12	0.580	58%	317468
	0.97	8.8	0.04	0.1	125ºC	24	0.720	72%	335119
	0.97	8.8	0.05	0.1	125ºC	6	0.581	58%	282227
Complex 3	0.97	8.8	0.05	0.1	125ºC	12	0.694	69%	323519
	0.97	8.8	0.05	0.1	125ºC	24	0.771	77%	346098

Antibacterial activity

The *in vitro* antibacterial activity of the ligands and complex **1-3** were tested using the agar well diffusion method. The growth inhibition zone was measured in diameter (mm) and the results are listed in Table 5. Standard antibacterial drug chloramphenicol was used as references to estimate the effectiveness of the tested compounds under the same conditions. The obtained results indicate that the complexes were more effective against *E. coli* under identical experimental conditions. It was observed that all complexes were more effective than Schiff base ligands. It was probably due to the established reason that chelation of Schiff base with metal ion enhances the lipophilicity of the central metal atom, which subsequently favours its permeation through the lipid layers of the cell membrane and blocking the metal binding sites on enzymes of microorganisms (Shukla *et al.,* 2015). Complex **1** has higher bacterial activity than the other complexes. The antibacterial activity of the ligands and their complexes are found in order: **1 > 2 > 3 > L_3 >L_2 > L_1.**

Table 5: Antibacterial screening data of ligands and complex 1-3 against *Escherichia Coli*

S. No.	Compounds	*Sensitivity	**Diameter of inhibition zone (in mm)
1.	Chloramphenicol	+	48±0.03
2.	L_1	+	24±0.5
3.	L_2	+	27±0.3
4.	L_3	+	28±0.6
5.	Complex 1	+	37±0.8
6.	Complex 2	+	34±0.7
7.	Complex 3	+	32±0.6

**Values as mean ±Standard Error Mean.*

Conclusion

This work describes the synthesis and characterization of three Schiff bases and their three Ti(IV) complexes. The geometries of the complexes were characterized by various spectroscopic methods and optimized by DFT calculations. The synthesized compounds were tested for catalytic activity in the synthesis of biodegradable polymer polycaprolactone from ε-caprolactone by ring-opening polymerization. Antibacterial activity of ligands and complexes indicates that activity of the ligand become more pronounced when coordinated with the metal ions. Hence, from all these extensive studies, it may be concluded that some of these complexes could be exploited for the design of novel antibacterial drug as well as catalytic material for polymerization reaction to synthesize a biodegradable polymer.

ACKNOWLEDGEMENT

The authors are grateful to **Principal,** Government Science College, Jabalpur and **Head**, Chemistry Department, for providing necessary laboratory facilities. We sincerely thankful to **SAIF CDRI** Lucknow, for recording elemental analysis, ESI-MS, ^{1}H-NMR, ^{13}C-NMR. One of us (Dimple Dehariya) is also grateful to the UGC-New Delhi for financial support through RGNF (Award letter no. F1-17.1/2013-14/RGNF-2013-14-SC-MAD-40702/(SA-III/Website).

REFERENCES

Aderoju AO, Ingo O and Oladunni MO (2012). Synthesis, spectroscopic, anticancer, and antimicrobial properties of some metal(II) complexes of (substituted) nitrophenol Schiff base. *International Journal of Inorganic Chemistry* 1-6.

Becke AD (1993). A new mixing of Hartree Fock and local density functional theories. *The Journal of Chemical Physics* **98(2)** 1372-1377.

Che CM and Huang JS (2003). Metal complexes of chiral binaphthyl Schiff base ligands and their application in stereoselective organic transformations. *Coordination Chemistry Reviews* **242** 97-113.

Chen HY, Tang HY and Lin CC (2006). Ring-Opening Polymerization of Lactides initiated by zinc alkoxides derived from NNO-tridentate ligands. *Macromolecules* **39** 3745-3752.

Chen HY, Tang, HY and Lin CC (2007). Ring-opening polymerization of L-lactide catalyzed by a biocompatible calcium complex. *Polymer* **48** 2257-2262.

Frisch MJ, Trucks GW, Schlegel HB, Scuseria GE and Robb MA (2010). Gaussian 09, Revision C.01, Gaussian, Inc., Wallingford CT.

Geary WJ (1971). The use of conductivity measurements in organic solvents for the characterization of coordination compounds. *Coordination Chemistry Reviews* **7(1)** 81-122.

Ha CS, and Gardella JA (2005). Surface Chemistry of Biodegradable Polymers for Drug Delivery Systems. *Chemical Reviews* **105** 4205-4232.

Hamil AM, Khalifa KM, AL-Houni A and El-ajaily MM (2009). Synthesis, Spectroscopic investigation and antiactivity activity of Schiff base complexes of cobalt(II) and copper(II) ions. *Rasayan Journal of Chemistry* **2(2)** 261-266.

Hung WC and Lin CC (2009). Preparation, characterization, and catalytic studies of magnesium complexes supported by NNO-tridentate Schiff base ligands. *Inorganic Chemistry* **48** 728-734.

Jeffery GH, Bassett J, Mendham J and Denney RC (1989). Vogel's Textbook of Quantitative Inorganic Analysis, 5thedn, (John Wiley & Sons, Inc, New York) 454-462.

Kamalakannan P and Venkappayya D (2002). Synthesis and characterization of cobalt and nickel chelates of 5-dimethylaminomethyl- 2-thiouracil and their evaluation as antimicrobial and anticancer agents. *Journal of Inorganic Biochemistry* **21** 22-37.

Lever ABP (1984). Inorganic Electronic Spectroscopy, 2nd Edn, Elsevier, New York

Lu WY, Hsiao MW, Hsu SCN, Peng WD, Chang YJ, Tsou YC, Wu TY, Lai YC, Chen Y and Chen HY (2012). Synthesis, characterization and catalytic activity of lithium and sodium iminophenoxide complexes towards ring-opening polymerization of L-lactide. *Dalton Transactions* **41** 3659-3667.

Maurya RC, Malik BA, Mir JM and Sharma AK (2014). Synthesis, characterization, thermal behaviour, and DFT aspects of some oxovanadium(IV) complexes involving ONO-donor sugar Schiff bases. *Journal of Coordination Chemistry* **67(18)** 3084-3106.

Parr RG, SzentpalyLv and Liu S (1999). Electrophilicity index. *Journal of the American Chemical Society* **121** 1922-1924.

Pelczar MJ, Chan ECS and Krieg NR (2001). *Text Book of Microbiology,* 5th edn (McGraw-Hill Publishing Company Ltd) New Delhi, India 138.

Platel RH, Hodgson LM and Williams CK (2008). Biocompatible initiators for lactide polymerization. *Polymer Reviews* **48** 11-63.

Silverstein RM, Bassler GC and Morrill TC (1991). Spectrometric Identification of Organic Compound. (John Wiley and Sons, Inc) New York 82-108, 123-131, 219-262.

Scozzafava A, Menabuoni L and Mincione F (2001). Carbonic anhydrase inhibitors: Synthesis of sulfonamides incorporating dtpa tails and of their zinc complexes with powerful topical antiglaucoma properties. *Bioorganic and Medicinal Chemistry Letters* **11** 575-582.

Scrocco E and Tomasi J (1978). Electronic Molecular Structure, Reactivity, and Intermolecular Forces: An Euristic Interpretation by Means of Electrostatic Molecular Potentials. in: *L. Per-Olov* (edn.), **11**, *Advances in Quantum Chemistry* 115-193.

Shukla SN, Gaur P, Mathews S, Khan S and Srivastava A (2008). Synthesis, characterization, catalytic and biological activity of some bimetallic selenocyanate Lewis acid derivatives of *N*, *N'-bis* (2-chlorobenzylidene)ethylenediamine. *Journal of Coordination Chemistry* **61** 3913-3921.
Shukla SN, Gaur P, Jhariya S, Chaurasia B, Vaidya P, Dehariya D, Azam M. (2018). Synthesis, Characterization, *In Vitro* Anti-diabetic, Antibacterial and Anticorrosive Activity of Some Cr(III) Complexes of Schiff Bases Derived from Isoniazid. *Chemical Science Transaction* **7(3)** 00-00.
Sujamol MS, Athira CJ, Sindhu Y and Mohanan K (2010). Synthesis, spectroscopic characterization, electrochemical behaviour and thermal decomposition studies of some transition metal complexes with an azo derivative. *Spectrochimica Acta, Part A***75** 106-112.
Badwaik VB and Aswar AS (2007). Synthesis, characterization, and biological studies of some Schiff base complexes. *Russian Journal of Coordination Chemistry* **33** 755-760.
Yamada S (1999). Advancement in stereochemical aspects of Schiff base metal complexes. *Coordination Chemistry Reviews* **190-192** 537-555.